Physical Environment

Ecosystem Indicators and Trends Used by FOCI - 2005

Edited by S. Allen Macklin, NOAA/PMEL

Last updated: September 2005

FOCI's scientists employ a number of climate, weather, and ocean indices and trends to help describe and ascribe the status of the ecosystem to various patterns or regimes. This document presents some of these with respect to current (2004) conditions. This section begins with an overview of North Pacific climate for 2004, including an examination of trends and tendencies in multidecadal and decadal climate regimes. Following this section are sections dealing explicitly with the western Gulf of Alaska and eastern Bering Sea. Within these are continuations of discussions begun in 2003 on eddy kinetic energy in the Gulf of Alaska and modeled drift trajectories for the Bering Sea.

Pacific Climate Overview – 2005

S. Rodionov, J. Overland, and N. Bond (NOAA PMEL)

Last updated: September 2005

Summary. *The winter of 2005 was characterized by atmospheric circulation anomalies that little resembled leading teleconnection modes. There was a weak El Niño event, but it had either a minor or atypical impact on the North Pacific. The PDO index was positive, suggesting that the climate regime established since the late 1970s still continues, but the distribution of sea surface temperature (SST) in the North Pacific did not closely correspond with the PDO loading pattern. The characteristic features of this distribution were a warm water pool in the east-central North Pacific and patchiness of SST anomalies elsewhere. The SST-based Victoria pattern, after being in its positive phase during 1999-2004, showed a sign of reversal in 2005. It was not consistent, however, with its atmospheric counterpart, a north-south dipole in sea level pressure (SLP). Instead, the anomalous SLP in 2005 featured an east-west dipole consisting of a negative anomaly centered along 170˚W from 40˚N into the Bering Sea, and a positive anomaly in the eastern Pacific from 40˚N into the Gulf of Alaska. This combination brought about southerly wind anomalies and an enhancement of cyclonic activity for the Bering Sea shelf, and a suppression of storminess in the eastern North Pacific.*

Climate in 2005

It is in the human nature to search for patterns, but it is difficult to characterize the winter of 2005 in terms of previously identified patterns of variability. In other words, it seems easier to describe this winter climate by what it was not. It was not a winter of a distinct El Niño-Southern Oscillation (ENSO) event. The distribution of sea-surface (SST) temperature anomalies in the North Pacific was neither the Pacific Decadal Oscillation (PDO), nor the Victoria patterns, and the Arctic Oscillation (AO) index was in the neutral phase, overall.

The Southern Oscillation Index (SOI) was negative in all months from June 2004 to June 2005, except January 2005 (Figure 1), and SST anomalies in the Niño 3.4 region in the central equatorial Pacific exceeded 0.5°C (Figure 2). It was enough to qualify as an El Niño event by some definitions, but it was in a weak category and accompanied by a number of uncharacteristic features. First, it did not extend all the way to West Coast of South America (Niño 1+2 region) where SST anomalies were predominantly negative (Figure 2). Second, there was a lack of persistent enhanced convection over the anomalously warm waters of the central equatorial Pacific, which has limited El Niño-related impacts on the global circulation patterns. For example, a weaker than average jet stream across the central and eastern Pacific in the winter of 2005 is inconsistent with El Niño.

The Aleutian low was stronger than normal and the PDO index, as expressed by the PC1 in Figure 3 (bottom panel), was positive, but the distribution of SST anomalies in the North Pacific (Figure 4) had little resemblance with the PDO loading pattern (Figure 3 upper panel). The characteristic features of this distribution in winter 2005 were a warm water pool in the east-central North Pacific and patchiness of SST anomalies elsewhere. Later, in spring and summer of 2005, the warm waters spread to the east, closer to the North American west coast, and negative SST anomalies in the western and central North Pacific became more pronounced. As a result, the whole pattern became much more like the positive phase of the PDO, and the PDO index values jumped above one standard deviation for the months from March through June.

The resemblance of the SST anomaly distribution in the winter of 2005 to the negative phase of the Victoria pattern (EOF2 in Figure 3) is somewhat greater than with the PDO, largely due to the heavy weight of the positive SST anomaly in the east-central North Pacific. The PC2 (EOF2) value in 2005 was negative for the first time since the shift in this pattern to the positive phase in 1999. The distribution of sea-level pressure (SLP) in the winter of 2005 (Figure 5), however, did not exhibit the north-south dipole pattern characteristic of the Victoria pattern. As in the previous seven years, SLP anomalies over the Bering Sea continue to be negative, indicating enhanced cyclonic activity there.

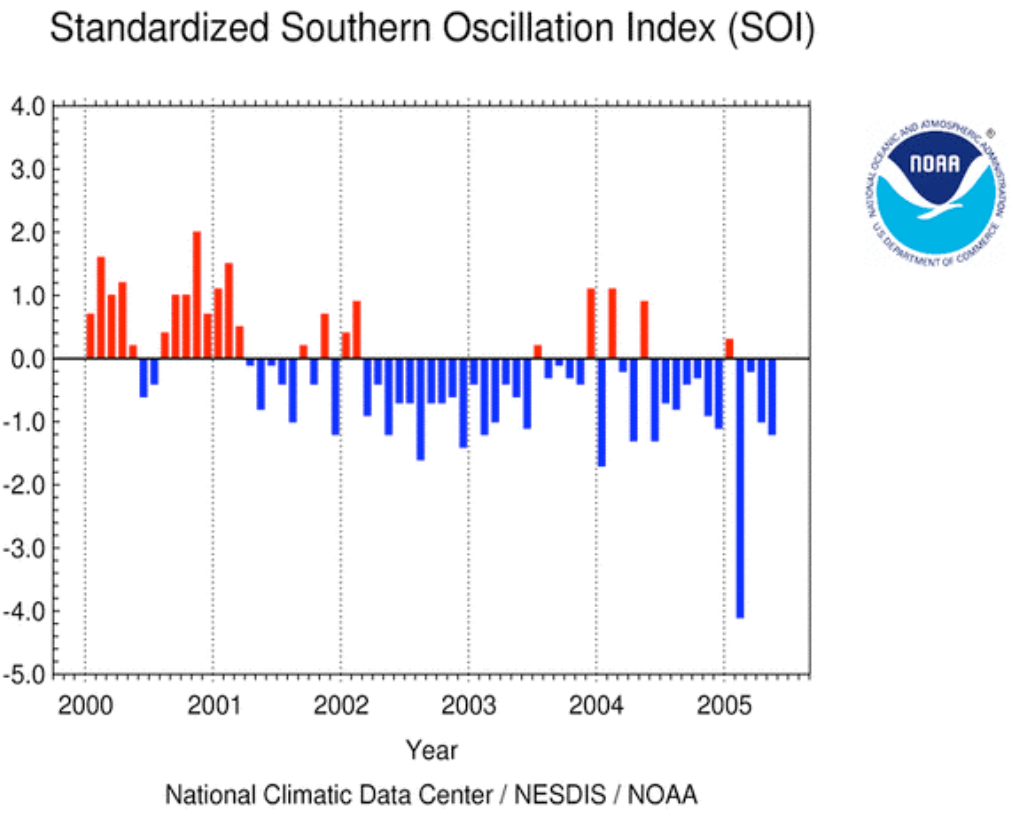

Figure 1. Mean monthly values of the Southern Oscillation Index, January 2000 through May 2005.

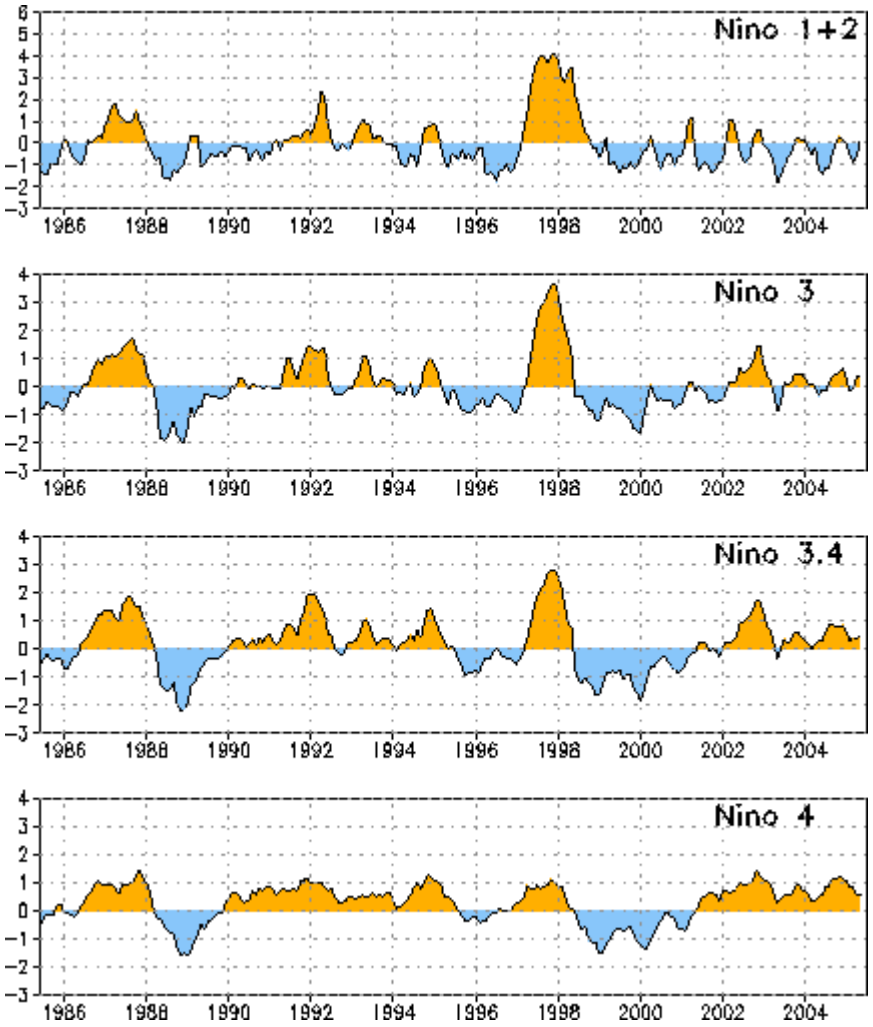

Figure 2. SST anomalies (deg. C) along the west coast of South America (Nino 1+2 region) and central parts of the equatorial belt (Nino 3, 3.4, and 4 regions), 1985-2005.

One of the most salient features of the atmospheric circulation over the North Pacific in the winter of 2005 was a strong and persistent high pressure cell off British Columbia. It split the North Pacific storm track redirecting storms either to the Bering Sea or southern California. During this winter, the Pacific Northwest (which includes Washington, Oregon, and Idaho) received only 6.23 inches of precipitation making it the fifth driest winter on record since 1896. In contrast, storms were bringing heavy rain to southern California triggering mudslides and washing away roads and runways. Los Angeles, for example, received a total of 19.58 inches of rain from December 2004 to February 2005, which makes this winter the forth wettest since 1945.

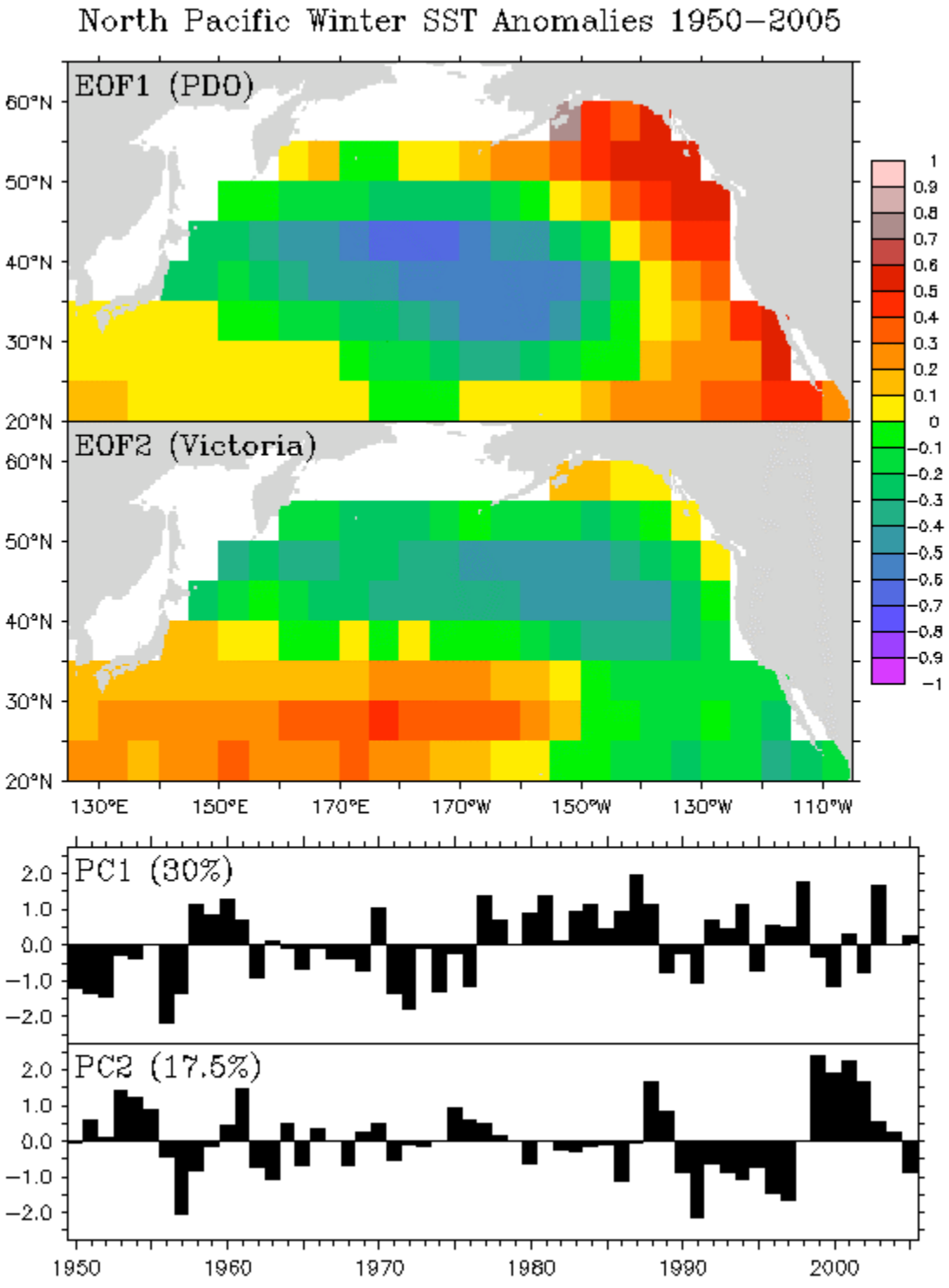

Figure 3. The first (PDO) and second (Victoria) empirical orthogonal functions of mean winter (Nov-Mar) SST anomalies in the North Pacific along with the time series of their principal components.

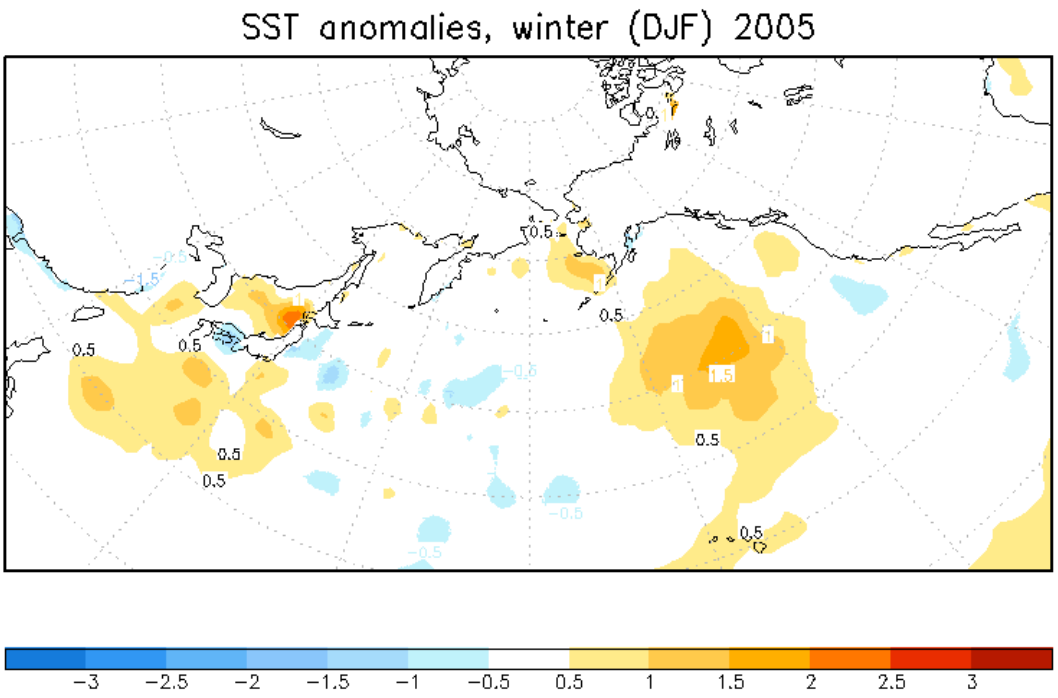

Figure 4. Mean seasonal SST anomalies in the winter (DJF) of 2005. Anomalies are relative to the 1971-2000 base period. Source data: NOAA OI.v2 SST monthly fields.

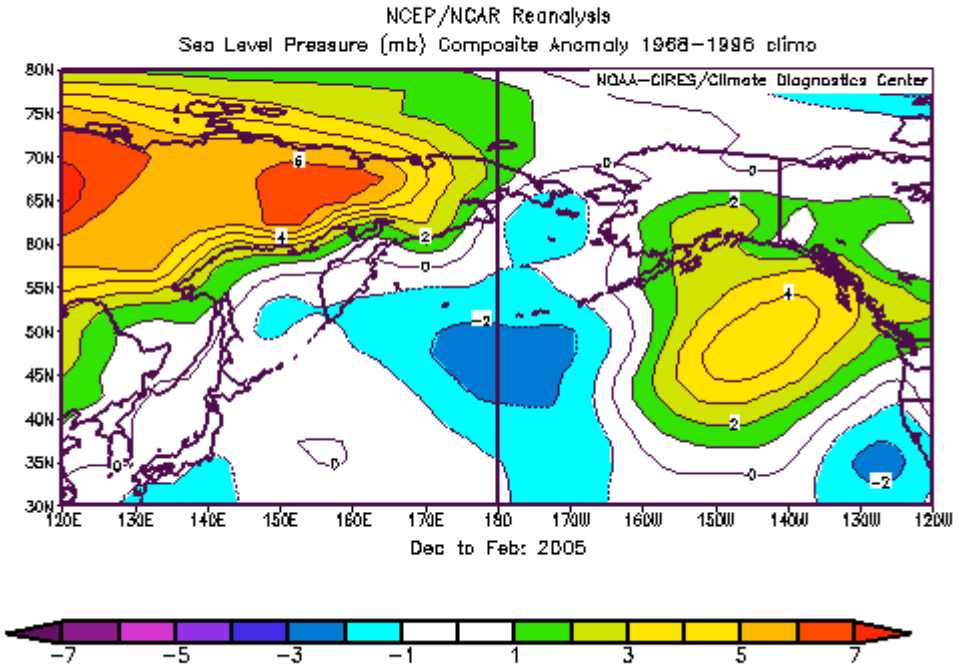

Figure 5. Mean seasonal SLP anomalies in the winter (DJF) of 2005. Anomalies are relative to the 1968-1996 base period.

The atmospheric circulation anomalies during the first half of 2005 appear to be linked to major disruptions in the marine ecosystem off the west coast of the U.S. The combination of higher than normal SLP to the northwest of Vancouver Island, and lower than normal SLP to the west of California during early 2005 (Figure 5) implies easterly wind anomalies, and in turn, anomalous poleward Ekman transports in the upper ocean off the coast of Oregon and Washington. This set of conditions was followed in spring and summer by lower than normal SLP off the U.S. west coast, leading to a delayed onset and a decreased intensity to coastal upwelling. The anomalous atmospheric forcing in winter and spring/early summer appears to have had substantial biological impacts in the northern portion of the California Current system, namely, a reduction in primary productivity, low zooplankton concentrations, and unusually high mortality rates for juvenile salmon and sea birds.

Recent Trends

The value of the winter PDO index in 2005 was close to the mean value of the index for the period since 1977 (Figure 6a). Although there were episodic excursions of the index into the negative territory, such as in 1989-1991 and 1999-2000, none of them materialized into a major regime shift similar in scale to those in the mid-1940s and late 1970s.

The summer (Figure 6b) and annual (Figure 6c) PDO index experienced a longer period of negative values since 1999, and there is the potential for a new regime shift. On the other hand, strongly positive values of the index in March-June 2005 suggest that the test for a regime shift based on the sequential algorithm (Rodionov 2005) will likely fail to support the regime shift in the late 1990s any longer.

Variations in the North Pacific Index (NPINCAR in Figure 6d, which measures the strength of the Aleutian low, is similar to those in the winter PDO index, particularly in the later part of the record. The correlation coefficient between the two is -0.72 for the period 1950-2005. The NPINCAR also shows no major regime shifts since 1977.

The lack of major regime shifts since the late 1970s does not mean that the climate remained the same throughout all this period. To investigate shorter-term, but sustained fluctuations in the system, the sequential method was applied to a number of climate indices, using a smaller cutoff length of 7 years. Figure 7a shows that the Aleutian low was the strongest for about a decade immediately following the regime shift in the late 1970s. Interestingly, the variability of the NPINCAR during that decade also increased. Occasional positive values of the index, however, did not seem to have had much effect on the North Pacific SST pattern, as expressed by the PDO index, which remained positive almost all this time (Figure 7b). In the late 1980s, the Aleutian low weakened substantially (the shift of 1988 is significant at $p = 0.02$), and the PDO index returned to its near-normal value. Later the Aleutian low strengthened again (the shift of 1996 is significant at $p = 0.04$), but not as much as in 1977-1987. The PDO index continued to fluctuate around its zero value until 2003, when it jumped to its highest value since 1941 signaling a possibility of a new regime shift.

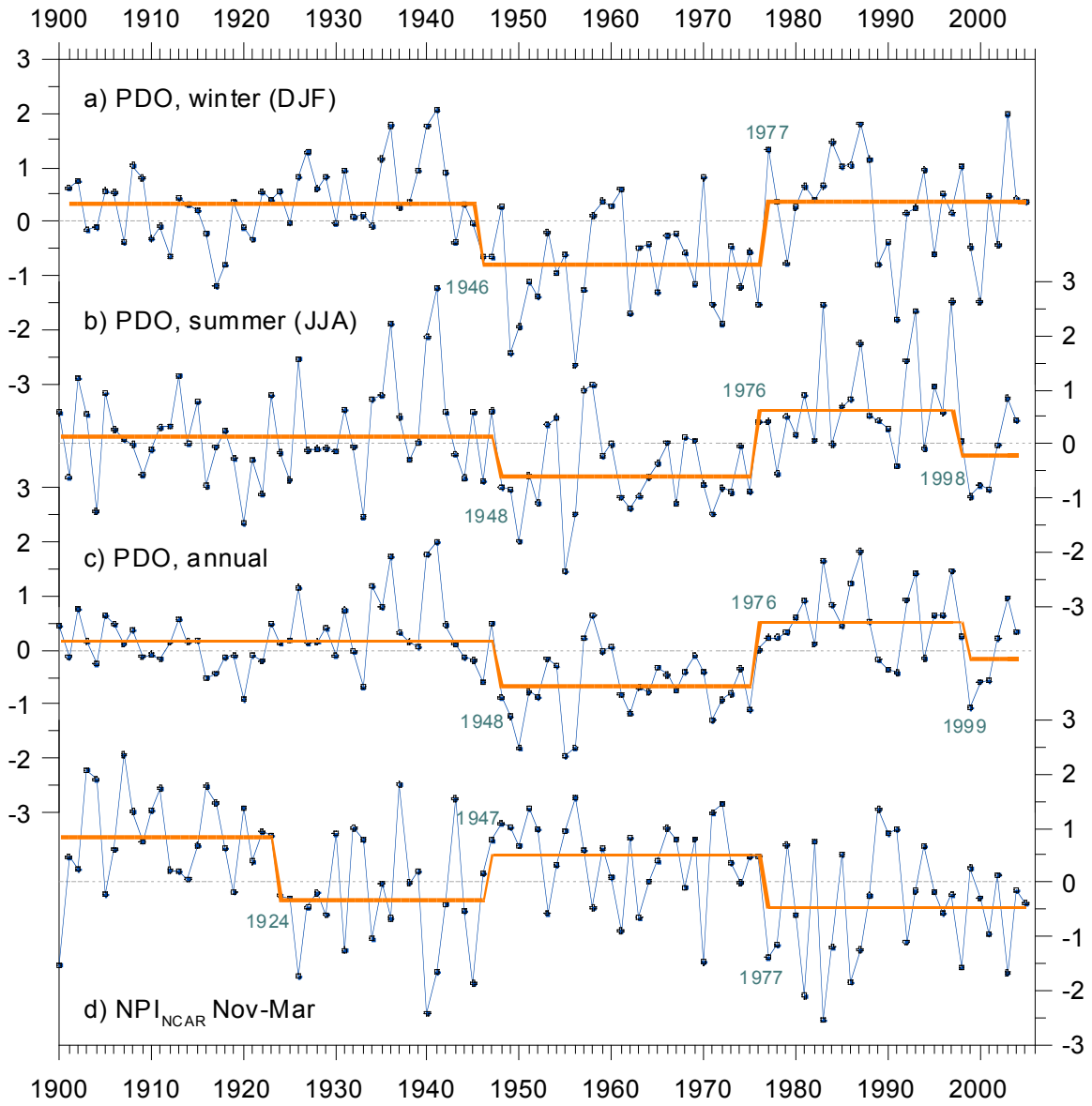

Figure 6. a) Mean winter (DJF) PDO index, 1901-2005, b) mean summer (JJA) PDO index, 1900-2004, c) Annual (Jan-Dec) PDO index, 1900-2004, and d) North Pacific index (Nov-Mar) from the National Center for Atmospheric Research, 1900-2005. The stepwise functions (orange lines) characterize regime shifts in the level of fluctuations of the indices. Shift points were calculated using the STARS method (Rodionov 2004), with the cutoff length of 15 years, the maximum significance level of 0.05, and the Huber weight function value of 1. The actual significance levels of the shifts are less than 0.0005.

The shift of the late 1980s was recorded in a number of fish stocks (McFarlane et al. 2000; Hare and Mantua 2000). As for the climate indices, the shift was particularly strong in the AO index that jumped to its record level in 1989 (Figure 7c). This state of highly positive AO index continued for 5 years. Since 1994 the index has fluctuated around its zero value.

Bond et al. (2003) argue that Pacific climate variability in recent years was associated primarily with the Victoria pattern, rather than with the PDO. This is clearly seen in Figure 3 (bottom

panel) where the PC1 (PDO) time series fluctuated around its zero value since the late 1980s, whereas the PC2 (Victoria) values were consistently negative in 1988-1997 and consistently positive in 1999-2004. To determine the atmospheric counterparts of the PDO and Victoria pattern, the PC1 and PC2 time series were correlated against geopotential height values at the 500-hPa level. Figure 8a shows that, over the North Pacific, the PDO is characterized by a dipole with the positive center at 15˚N, 180 and the negative center at 45˚N, 165˚W. This dipole practically coincides with the oceanic centers of the Pacific/North American (PNA) pattern. The atmospheric counterpart of the Victoria pattern is also a dipole with the centers at 30˚N, 165˚W and 60˚N, 165˚W (Figure 8b). The Victoria dipole is, practically, in quadrature with the PDO dipole.

The atmospheric PDO and Victoria indices are presented in Figure 7d and Figure 7e, respectively. The indices are calculated as the normalized differences in 500-hPa height anomalies in the positive and negative centers of the respected dipoles. The atmospheric PDO index correlates with its oceanic counterpart at $r = 0.83$; it also exhibits shifts in 1977 and 1989, but not in 2003. The correlation coefficient between the atmospheric and oceanic Victoria indices is $r = 0.78$. The regime of negative index values in 1990-1997, which is clearly seen in PC2 time series (Figure 3), is not statistically significant in the atmospheric Victoria index. The only statistically significant regime-like feature in the latter index is a sequence of positive values in 1998-2002. Neither the PDO nor the Victoria indices can fully explain an abrupt shift to warmer conditions in the Bering Sea since 2000 (see the Bering Sea section).

In order to capture the part of atmospheric circulation in Figure 5 relevant to the Bering Sea, we calculated an index that represents a difference in SLP between two areas, 45-60˚N, 130-150˚W and 40-65˚N, 160-180˚W, normalized by its standard deviation. The positive (negative) values of this East-Central North Pacific (ECNP) index indicate positive (negative) east-west SLP gradient and predominantly southerly (northerly) winds over east-central North Pacific and the Bering Sea. The ECNP index does not correlate with the PDO or the Victoria indices. It is interesting, however, that all 20 positive values of the index since 1970 coincide with positive values of either the PDO or Victoria indices. It is important to underscore that the ECNP index does not represent a major mode of climate variability, such as the PDO or Victoria patterns. Instead, it appears to capture the essential elements of both these patterns pertinent to warming in the Bering Sea. The time series of the ECNP index for January-February is shown in Figure 7. The index is almost the same if averaged over the entire winter season, December through March. However, the shift in 2000 is most significant for the January-February index. As shown in the Bering Sea section, this year marks the beginning of a warm period in the sea.

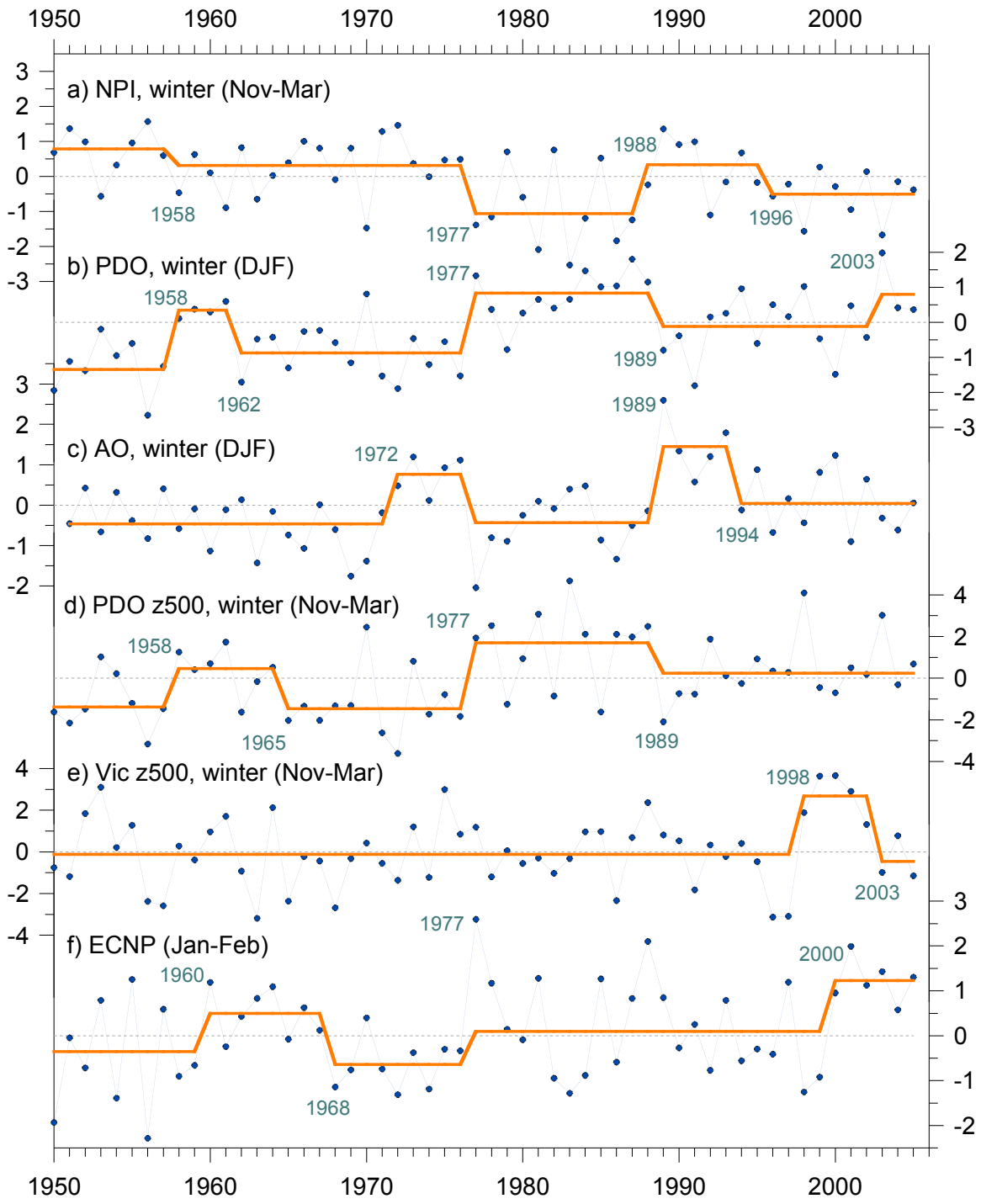

Figure 7. a) Mean winter (Nov-Mar) NPINCAR, 1950-2005, b) Mean winter (DJF) PDO index, 1950-2005, c) Mean winter (DJF) Arctic Oscillation index, 1951-2005, d) Mean winter (Nov-Mar) atmospheric PDO index at the 500-hPa level, 1950-2005, e) Mean winter (Nov-Mar) atmospheric Victoria index at the 500-hPa level, 1950-2005, and f) January-February East-Central North Pacific index, 1950-2005. The stepwise functions (orange lines) characterize regime shifts in the level of fluctuations of the indices. Shift points were calculated using the STARS method (Rodionov 2004), with the cutoff length of 7 years, the maximum significance level of 0.2, and the Huber weight parameter of 1.

a) R [PC1 (PDO) vs. z500]

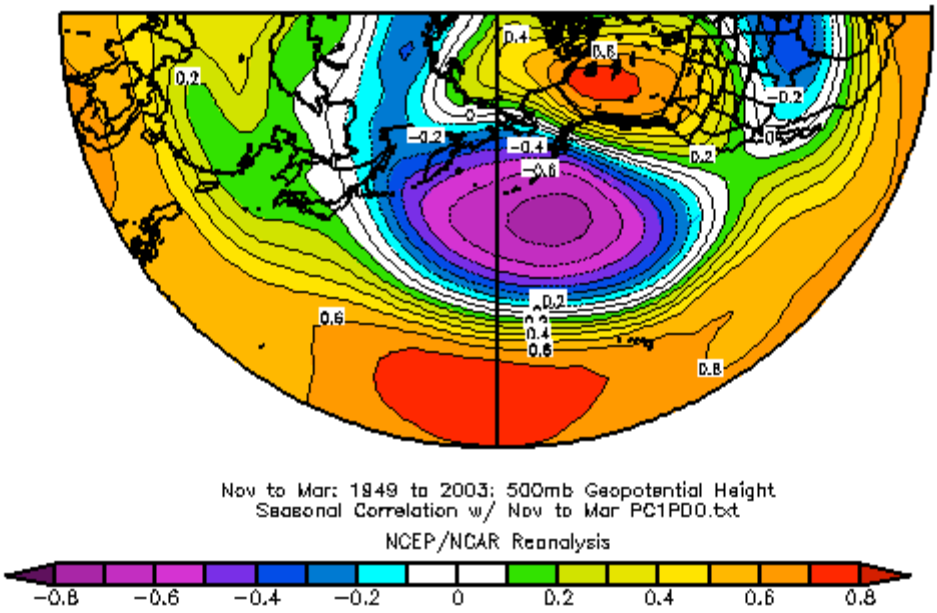

b) R [PC2 (Victoria) vs. z500]

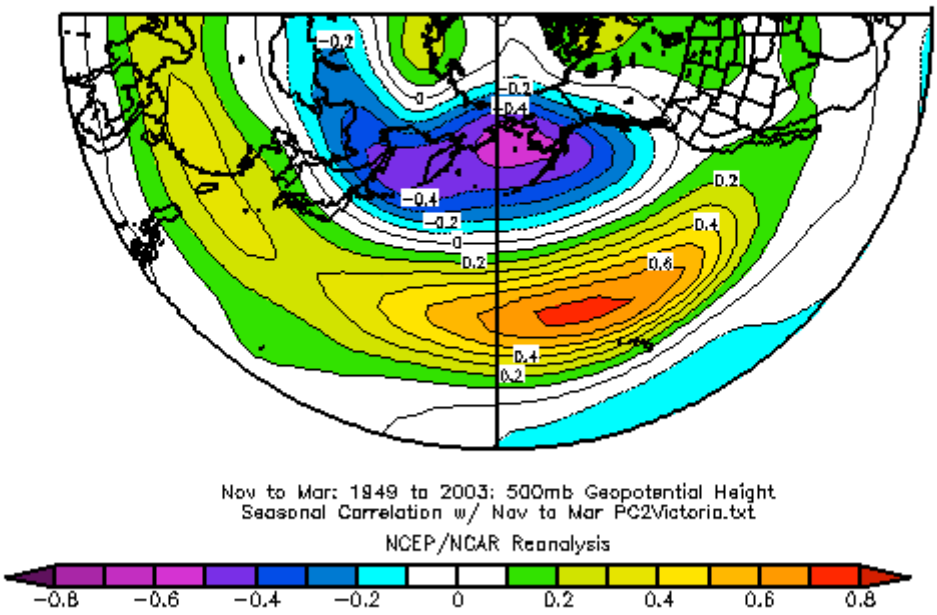

Figure 8. Correlation coefficients between mean winter (Nov-Mar) 500-hPa heights at grid points with (a) PC1 (PDO) and (b) PC2 (Victoria) time series from Figure 3.

It has been shown that the North Pacific atmosphere-ocean system included anomalies during the winter of 2004-05 that were unlike those associated with the primary modes of past variability. This result suggests a combination of two factors: (1) that the nature of North Pacific variability is actually richer in variability than appreciated previously, and (2), that there is the potential for significant evolution in the patterns of variability due to both random, stochastic effects and

systematic trends such as global warming. Notably, at the time of this writing, it cannot be determined whether the North Pacific is heading into a positive PDO-like condition or some other state.

GULF OF ALASKA

Pollock Survival Indices –FOCI

Contributed by S. A. Macklin, NOAA/PMEL
Last updated: September 2005

Using a conceptual model of early-life survival of western Gulf of Alaska walleye pollock (Megrey et al. 1996) for guidance, FOCI maintains several annual environmental indices. The indices are formulaic elements of a yearly prediction, during the year the fish are spawned, of the number of fish that will recruit as two-year olds. Some indices are determined qualitatively; the two reported here, seasonal rainfall at Kodiak and wind mixing in the exit region of Shelikof Strait, are determined numerically. Although data sources have changed somewhat over the years, chiefly with information used to estimate wind-mixing energy, every effort has been expended to make interannual comparisons accurate and reliable.

Presently, the FOCI program is developing a modified approach (Megrey et al. 2005) to its annual forecast algorithm. When modifications are complete, it is probable that new indices will become available for this report. It is possible that the indices presented here and in past years may be discontinued. Until a significantly long time series of new annual indices is available, the old indices will continue to be updated and published in this report.

Seasonal rainfall at Kodiak

FOCI uses measured Kodiak rainfall as a proxy for freshwater discharge that promotes formation of baroclinic instabilities (eddies) in the Alaska Coastal Current (ACC) flowing through Shelikof Strait (Megrey et al. 1996). The amount of measured monthly rainfall drives a simple model that produces an index of survival for age-0 walleye pollock. These young fish may benefit from spending their earliest developmental stages within eddies (Schumacher and Stabeno 1994). The model assumes that greater-than-average late winter (January, February, March) precipitation produces a greater snow pack. When the snow melts during spring and summer, it promotes discharge of fresh water through rivers and streams into the ACC. Similarly, greater than average spring and early summer rainfall, with nearly immediate run-off, also favors increased baroclinity after spawning. Conversely, decreased rainfall is likely detrimental to pollock survival because they do not find the circulation features that promote their survival.

The time series of FOCI's pollock survival index based on measured precipitation is shown in Figure 9. Although there is large interannual variability, a trend toward increased survival potential is apparent from 1962 (the start of the time series) until the mid 1980s. Since then, the survival potential has been more level. Survival potential increased in 2003 and 2004 because almost all winter and spring months experienced average or greater rainfall than their respective 30-year averages. In 2005, precipitation remained somewhat above average but less so than in the previous two years. Thus, the 2005 pollock survival potential based on precipitation, alone, is a bit less than in 2004, although still in the category of "average to strong" recruitment. Interestingly, the precipitation-based survival index does not appear to track any of the long-term climate indices (e.g., Arctic Oscillation (AO) index, Pacific Decadal Oscillation (PDO)) with any

consistency, possibly because of the way winter and spring precipitation are used in the model. In the 3-yr running mean of the precipitation survival index, there is a change from decreasing to increasing survival potential in 1989. In that year, there was an abrupt shift in the AO.

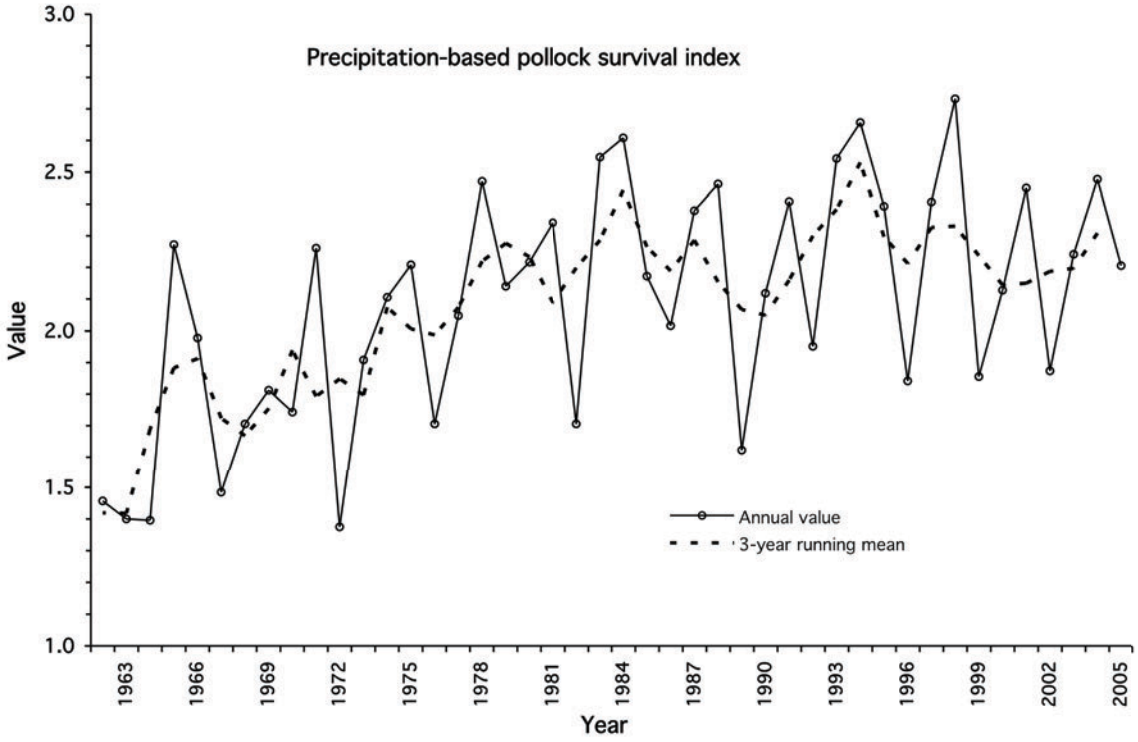

Figure 9. Index of pollock survival potential based on measured precipitation at Kodiak from 1962 through 2005. The solid line shows annual values of the index; the dashed line is the 3-year running mean.

Wind mixing at the southwestern end of Shelikof Strait

Rainfall is only one indicator of early-life-stage pollock survival. FOCI hypothesizes that a series of indices (proxies for environmental conditions, processes and relationships), assembled into a predictive model, provides a method for predicting recruitment of walleye pollock. A time series of wind mixing energy (W m^{-2}) at [57°N, 156°W] near the southern end of Shelikof Strait is the basis for a survival index wherein stronger than average mixing before spawning and weaker than average mixing after spawning favor survival of pollock (Megrey et al. 1996). The wind-mixing index is produced from twice-daily surface winds created from a model (Overland et al. 1980) using NCEP reanalyzed sea-level-pressure fields. The model is tuned to the region using information determined by Macklin et al. (1993). A time series of the wind-mixing index is shown in Figure 10. As with precipitation at Kodiak, there is wide interannual variability with a less noticeable and shorter trend to increasing survival potential from 1962 to the late 1970s. Recent survival potential has been high relative to the early years of the record. Except for March 2003 and March 2005, monthly averaged wind mixing in Shelikof Strait has been below the 30-

year (1962-1991) mean for the last eight January through June periods (1998-2005). This may be further evidence that the North Pacific climate regime has shifted in the past decade.

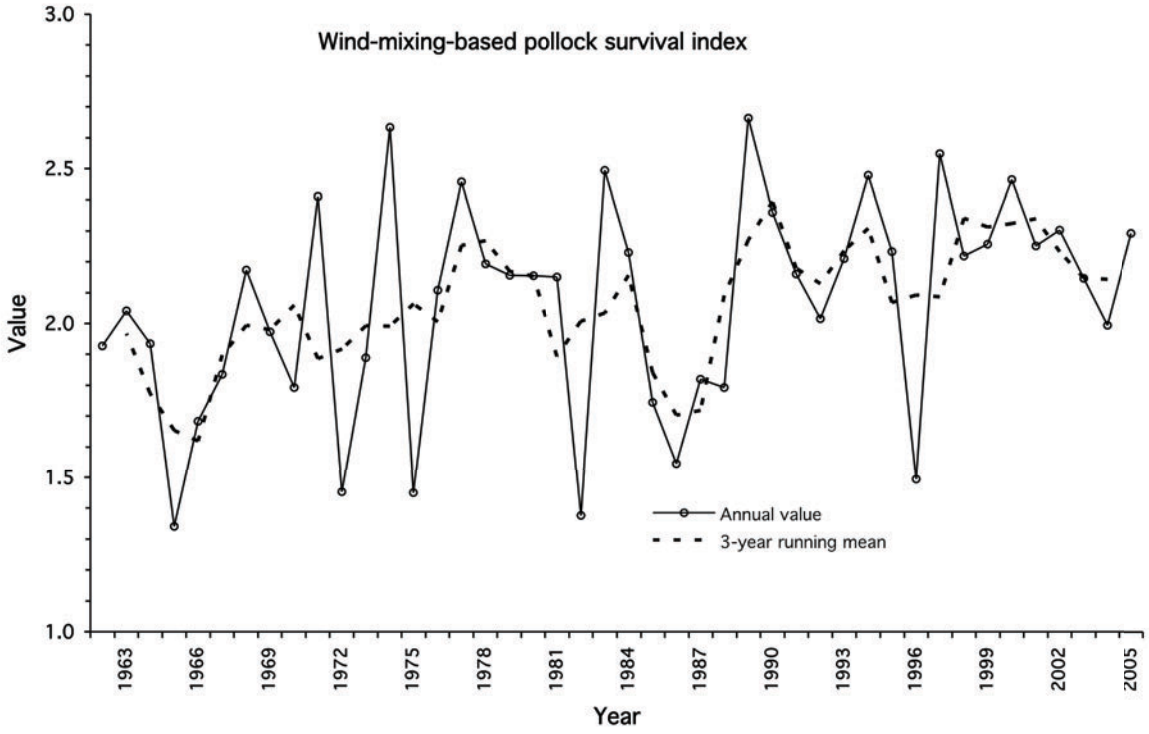

Figure 10. Index of pollock survival potential based on modeled wind mixing energy at [57°N, 156°W] near the southwestern end of Shelikof Strait from 1962 through 2005. The solid line shows annual values of the index; the dashed line is the 3-year running mean.

Ocean transport in the western Gulf of Alaska –FOCI
Contributed by P. J. Stabeno, NOAA/PMEL
Last updated: November 2003

The spring and summer seasonal strength of the Alaskan Stream and Alaska Coastal Current (ACC) is an important factor for overall productivity on the shelf of the Gulf of Alaska. FOCI uses satellite-tracked drift buoys, drogued at mid mixed-layer depths (~45 m), to measure ocean currents as a function of time and space. Animations of drifter trajectories from deployments during 2001-2003 can be found at *http://www.pmel.noaa.gov/steller/ssl_drifters.shtml*. There is a strong seasonal signal in the ACC. During late spring and summer, the flow on the Gulf of Alaska shelf between Prince William Sound and the Shumigan Islands is weak. The many bathymetric features such as troughs and banks interact with the currents. This results in flow up the eastern side of such troughs as Amatouli, Chiniak and Barnabas. Flow over banks such as Portlock, is often recirculating, and satellite-tracked drifters can be retained in closed circulation for weeks to months. ACC flow in the western Gulf of Alaska during 2001 and 2002 was particularly weak. Later in the summer or fall, with the intensification of regional winds, the

ACC becomes stronger, and the flow down Shelikof Strait becomes more organized, as shown by the animations for September of 2001 and 2002. During 2003 (Figure 11), ACC flow was more organized and stronger. Specifically, the flow in Shelikof Strait appeared more complex with more meanders and eddies than have been evident in previous years. This year, more than the typical number of drifters went aground along the Alaska Peninsula and the Kenai Peninsula west of Gore Point.

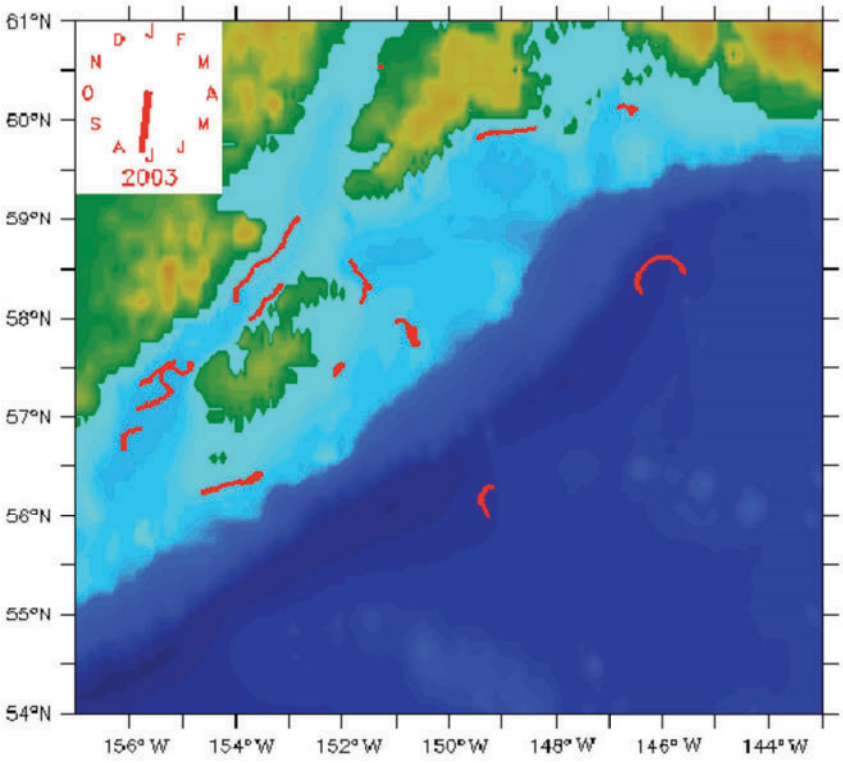

Figure 11. Tracks of satellite-tracked drifters for the period October 14-18, 2001, show sluggish flow on the shelf, except for within Shelikof Strait.

Cross-shelf fluxes are important to providing nutrients to the shelf. Each year (2001-2003) brought flow onto the shelf in the vicinity of the Seward Line, which extends south southeastward from the mouth of Resurrection Bay across the shelf and over the basin. The presence of an eddy is clearly evident from drift trajectories over the basin. Such eddies interact with the shelf, often drawing water off the shelf and into the basin, and are discussed in more detail in the next section. From the head of the gulf to Amchitka Pass, the Alaskan Stream appeared to be fairly typical during 2003, through July, with low eddy kinetic energy and relatively high velocity (>50 cm s^{-1} to the southwest). By next year, there will be enough data to allow construction of an annual Gulf of Alaska transport index that can be compared with climate indices such as PDO, AO, etc.

Eddies in the Gulf of Alaska – FOCI
Contributed by Carol Ladd, NOAA/PMEL
Last updated: September 2005

Eddies in the northern Gulf of Alaska have been shown to influence distributions of nutrients (Ladd et al. 2005) and phytoplankton biomass (Brickley and Thomas 2004) and the foraging

patterns of fur seals (Ream et al. 2005). Eddies propagating along the slope in the northern and western Gulf of Alaska are generally formed in the eastern gulf in the autumn or early winter (Okkonen et al. 2001). In most years, these eddies impinge on the shelf east of Kodiak Island in the spring. Using altimetry data from 1993 to 2001, (Okkonen et al. 2003) found an eddy in that location in the spring of every year except 1998. They found that strong, persistent eddies occur more often after 1997 than in the period from 1993 to 1997.

Since 1992, the Topex/Poseidon/Jason/ERS satellite altimetry system has been monitoring sea surface height (SSH). Gridded altimetry data (merged TOPEX/Poseidon, ERS-1/2, Jason and Envisat; Ducet et al. 2000) allow the calculation of eddy kinetic energy (EKE). A map of eddy kinetic energy in the Gulf of Alaska averaged over the altimetry record shows three regions local maxima (labeled a, b, and c in Figure 12). The first two regions are associated with the formation of Haida eddies (a) and Sitka eddies (b). Regions of enhanced EKE emanating from the local maxima illustrate the propagation pathways of these eddies. Sitka eddies can propagate southwestward (directly into the basin) or northwestward (along the shelf break). The Sitka eddies that follow the northwestward path often feed into the third high EKE region (c; Figure 12). By averaging EKE over region c (see box in Figure 12), we obtain an index of energy associated with eddies in this region (Figure 13).

Figure 12. Sea surface height anomaly from TOPEX/Poseidon, ERS-1/2 and Jason merged altimetry. Positive anomalies imply anticyclonic circulation. Black box outlines region over which EKE was averaged for Figure 13.

The seasonal cycle (calculated from the entire time series) of EKE averaged over the box shown in Figure 12 exhibits high EKE in the spring (March – May) with lower EKE in the autumn (September – November). EKE has been high with a stronger seasonal cycle since 1999. Prior to 1999, EKE was generally lower than the ~13-year average, although 1993 and 1997 both showed periods of high EKE. Interestingly, the first 8 months of 2005 showed a return to the low EKE values observed prior to 1999. No significant eddies were observed in this region during the first half of 2005. This may have implications for the ecosystem. Phytoplankton biomass was probably more tightly confined to the shelf during this time period due to the absence of eddies.

If fur seals have become dependent on eddies for foraging over the last five years of strong eddy variability, their foraging success may be negatively impacted this year. In addition, cross-shelf transport of heat, salinity and nutrients are likely to be smaller than in previous years with large persistent eddies. Research is ongoing as to the causes and implications of these patterns.

The altimeter products have been produced by the CLS Space Oceanography Division; downloaded from http://www.aviso.oceanobs.com/.

Figure 13. Eddy kinetic energy (EKE) averaged over the region shown in Figure 12 calculated from altimetry. Black: weekly EKE. Red: mean over entire time series. Green: annual cycle.

EASTERN BERING SEA - 2005

Temperature and Ice Cover - FOCI

S. Rodionov, P. Stabeno, J. Overland, N. Bond, and S. Salo, PMEL/NOAA
Last updated: September 2005

Summary. *The anomalously warm winter of 2005 follows similarly warm winters of 2003 and 2004. Although surface air temperature in the winter of 2002 was colder than 1961-2000 average, the depth-integrated temperatures at Mooring 2 indicate that the shift to warmer conditions in the Bering Sea began in the spring of 2000. This warming becomes comparable in its scale with major warm episodes in the late 1930s and late 1970s – early 1980s. The spring transition is occurring earlier, and the number of days with ice cover after March 15 has a significant downward trend. In 2005, the ice cover index reached the record low value. The lack of ice cover over the southeastern shelf during recent winters resulted in significantly higher heat content in the water column. Sea surface temperature in May 2005 was above its long-term average value, which means that the summer bottom temperatures will likely be also above average.*

The winter of 2005 in the Bering Sea was anomalously warm, with the mean winter (DJFM) surface air temperature (SAT) at St. Paul being 2.34°C (or 1.4 standard deviations) above the 1961-2000 average. This increases our confidence that a shift toward a warmer climate in the Bering Sea occurred in 2001 (Figure 14a). The significance level for this shift is 0.09, which is based on the two-tailed Student t-test for the difference in the mean SAT values for the periods 1990-2000 and 2001-2005. This difference would have been even more statistically significant if there were no "outliers", specifically, a cold winter in 2002, and a warm winter in 1996. In response to this warming, the Bering Sea is experiencing a northward biogeographical shift (Overland and Stabeno 2004). If this shift continues over the next decade, it will have major impacts on commercial and subsistence harvests as Arctic species are displaced by sub-Arctic species.

Milder winters in the Bering Sea can partly be explained by the tendency for anomalously low SLP (Figure 14b), which indicates an enhanced cyclonic activity and increased advection of warm Pacific air. The level of cyclonic activity over the Bering Sea is linked to the strength of the Aleutian low, but it can also be associated with the north-south dipole of the Victoria pattern. The shift in Bering Sea pressure index (BSPI) in 1977 reflects the basin-wide climate shift and strengthening of the Aleutian low. The 1989 and 1998 shifts in the BSPI appear to be mostly a response to phase shifts in the Victoria pattern. In addition to cyclonic activity, an important factor responsible for thermal conditions in the Bering Sea is the mean meridional flow in the lower troposphere. As discussed in the Pacific section of the report, the East-Central North Pacific (ECNP) index (which takes into account both these factors) showed a statistically significant increase since 2000, suggesting greater Pacific influence on the Bering Sea.

This recent warming in the Bering Sea is not confined to the winter season. Figure 15a shows monthly SAT anomalies at St. Paul for the period from January 1995 through May 2005. Note the sharp transition from very low temperatures in the early winter of 2000 to anomalously warm conditions in late winter and spring of that year. Similar transitions, to a lesser degree, were observed in winter-spring of 1998 and 2002. Stabeno and Overland (2001) argue that the Bering Sea appears to have shifted toward a pattern of earlier spring transition. Since March 2002, SAT anomalies remained positive for 37 consecutive months until April 2005, which was slightly colder than normal. This is the longest run of positive SAT anomalies during the period of record extending back to 1916.

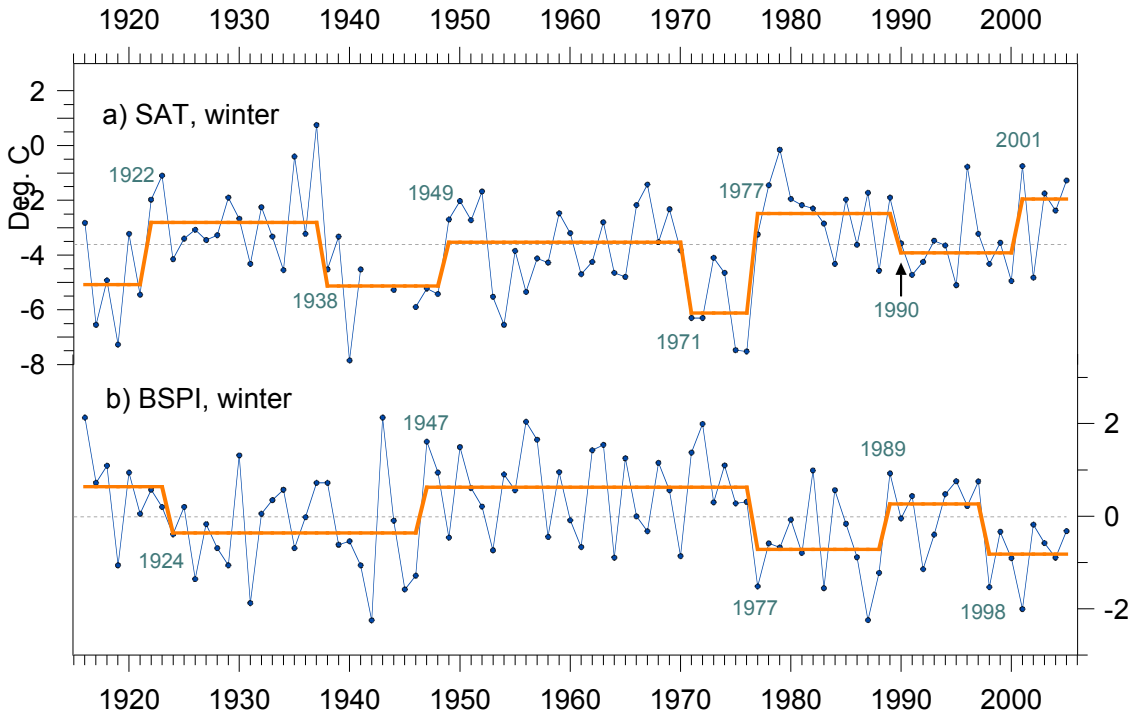

Figure 14. Mean winter (DJFM) a) surface air temperatures in St. Paul, Pribilof Islands and b) Bering Sea pressure index. The dashed line for the top graph indicates the mean SAT value of -3.62˚C for the base period, 1961-2000. Positive (negative) values of BSPI suggest anticyclonic (cyclonic) conditions in the Bering Sea. The stepwise functions (orange lines) characterize regime shifts in the level of fluctuations of the variables. Shift points were calculated using the sequential method (Rodionov 2004), with the cutoff length of 10 years, significance level of 0.2, and Huber weight parameter of 1. The latter reduces the effect of "outliers", if they exceed one standard deviation from the mean value of the corresponding regime.

To put this recent warmth in perspective, we calculated mean monthly SAT anomalies for the entire record since 1916 and smoothed them with 13-mo averages (Figure 15b). It is clear from this time series that the magnitude of the recent warmth is comparable with the major warm episodes in the 1930s and immediately after the regime shift in the late 1970s.

Figure 15b also shows three multidecadal regimes in SAT fluctuations: 1921-1939 (warm), 1940-1976 (cold), and 1977-2005 (warm). It is worth noting that the two previous regimes had a similar pattern, when SAT anomalies were strongest at the end of the regime, right before the system switched to a new one. In the current warm regime, the magnitude of SAT fluctuations has been steadily increasing since the mid-1980s, and the Bering Sea may become even warmer before it will switch to a new cold regime. If the regime concept is true, this switch may happen anytime soon, especially given the uncertain state of the North Pacific climate, suggesting that it may be in a transition phase (see the Pacific Climate overview section).

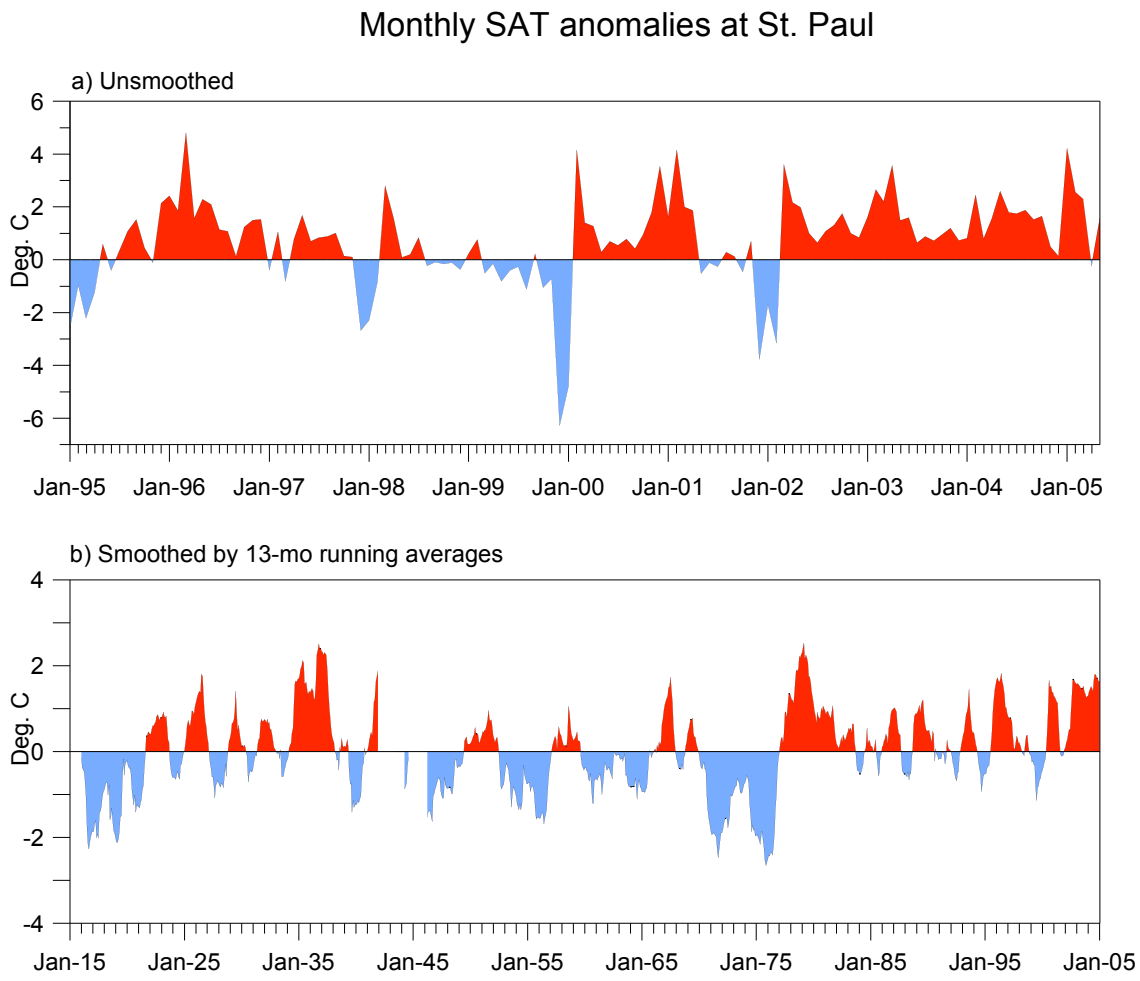

Figure 15. Mean monthly surface air temperatures anomalies in St. Paul, Pribilof Islands, a) unsmoothed, January 1995 through May 2005, and b) smoothed by 13-mo running averages and referred to the central month of the window, January 1916 through January 2005. The base period for calculating anomalies is 1961-2000.

An increase in year-to-year variability since the mid-1980s can also be seen in the Ice Cover Index (ICI, Figure 16a). In 2001, the ice cover index (ICI) plunged to a record low value, and then a new record was set in 2005.

As Figure 16b illustrates, there is a clear overall downward trend in the ice retreat index (IRI). The IRI represents the number of days with ice cover after March 15 in the 2˚ x 2˚ box (56-58°N, 163-165°W) that includes Mooring 2 (57°N, 164°W). Since the early 1970s, the index is declining at an average rate of almost 1 day per year, a trend significant at the 95% level. In the season of 2005, ice was practically absent in the box. A brief cold spell in April did bring about ice barely above the 10% threshold (Figure 17). This threshold is used to calculate the beginning and end of ice season (Figure 18). Based on this definition, the 2005 ice season lasted only 5 days. Similarly short ice seasons (less than 2 weeks) were observed in 2001 and 2003. In 2000 and 2002, in contrast, ice arrived to the vicinity of Mooring 2 very early, about one month prior to the average date for the beginning of ice season on January 14. Note, however, that starting with

the 1996 ice season, if ice arrives early, it retreats early too (with the exception of 1999). This supports the shift in the Bering Sea toward earlier spring transition (Stabeno and Overland 2001).

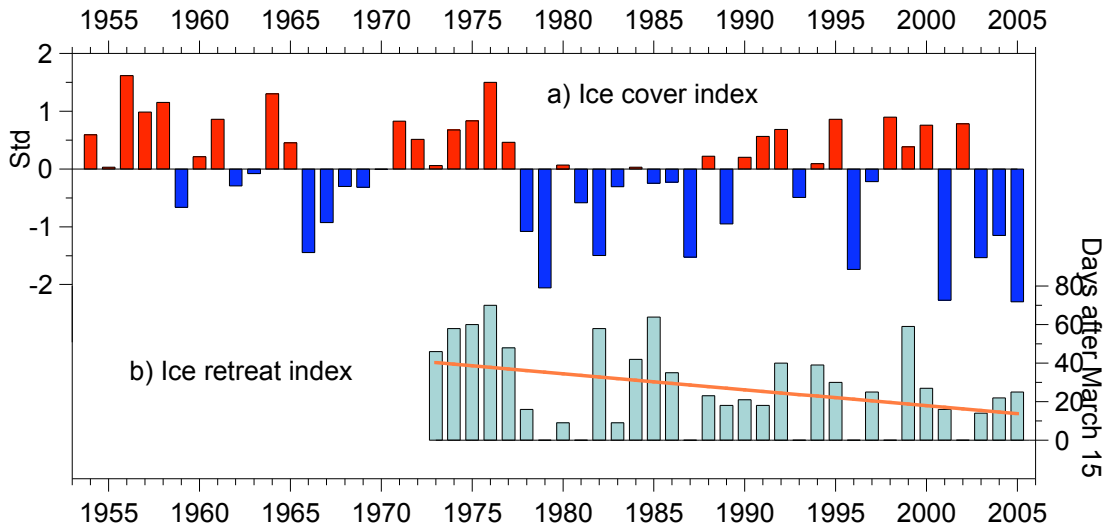

Figure 16. a) Ice cover index, 1954-2005, and b) ice retreat index and its linear trend (orange line), 1973-2005.

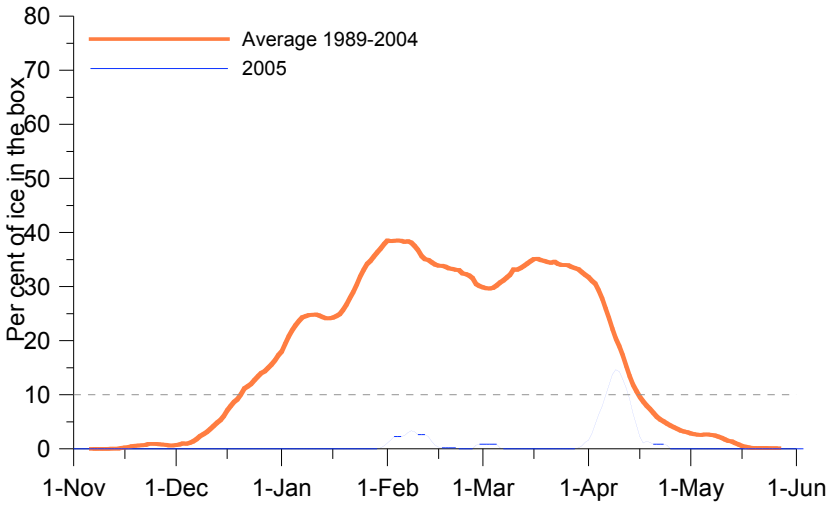

Figure 17. Percentage of ice cover in the 2˚ x 2˚ box (56-58°N, 163-165°W) during the winter of 2005.

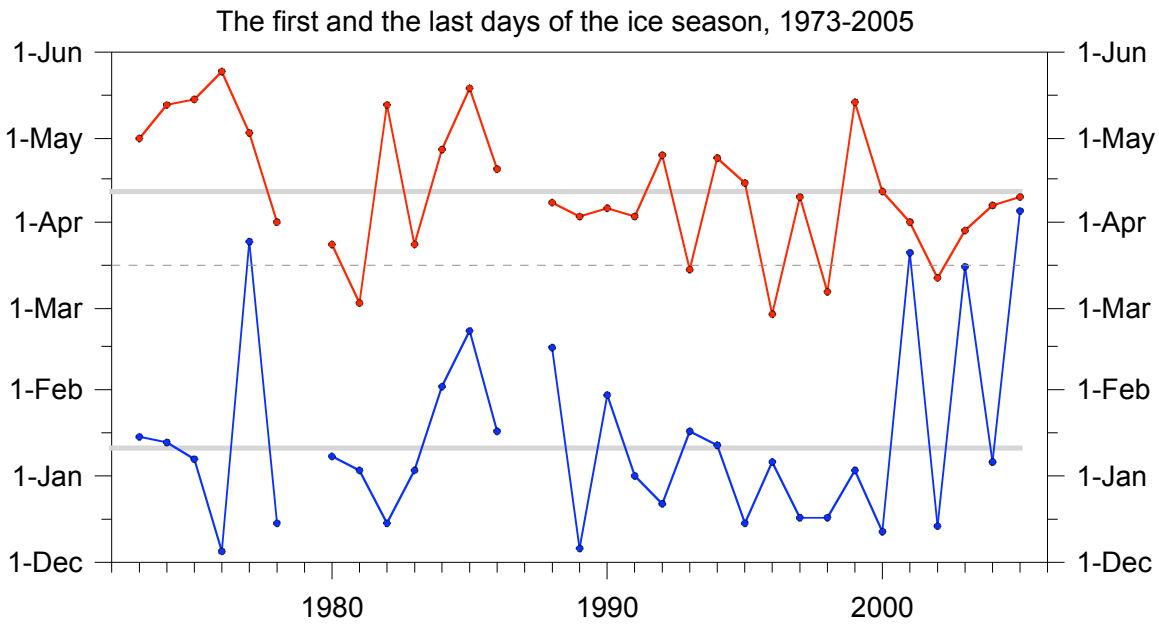

Figure 18. The first and last days of the ice season, 1973-2005. The gray solid horizontal lines are the mean dates for these two variables. The dashed line (March 15) is used as a threshold to calculate the ice retreat index. No ice was present in the box in 1979 and 1987.

The decrease in sea ice directly impacts water column temperature and salinity, and the timing of the spring bloom. These changes can be seen clearly in the data collected at two sites, Mooring 2 and Mooring 4 (Figure 19). The very cold temperatures (indicated by black) are accompanied by the *in situ* melting of ice. Generally, stratification develops during April. The water column exhibits a well-defined two-layer structure throughout the summer consisting of a 15-25 m wind mixed layer and 35-40 m tidally mixed bottom layer. When the bottom temperature is less than 2˚C, by definition it represents a "cold pool". In earlier years (1995, 1996, 1997, and 1999) bottom temperatures were below the 2˚C threshold, but in more recent years the temperatures are much warmer, indicating the failure of the formation of the southern cold pool.

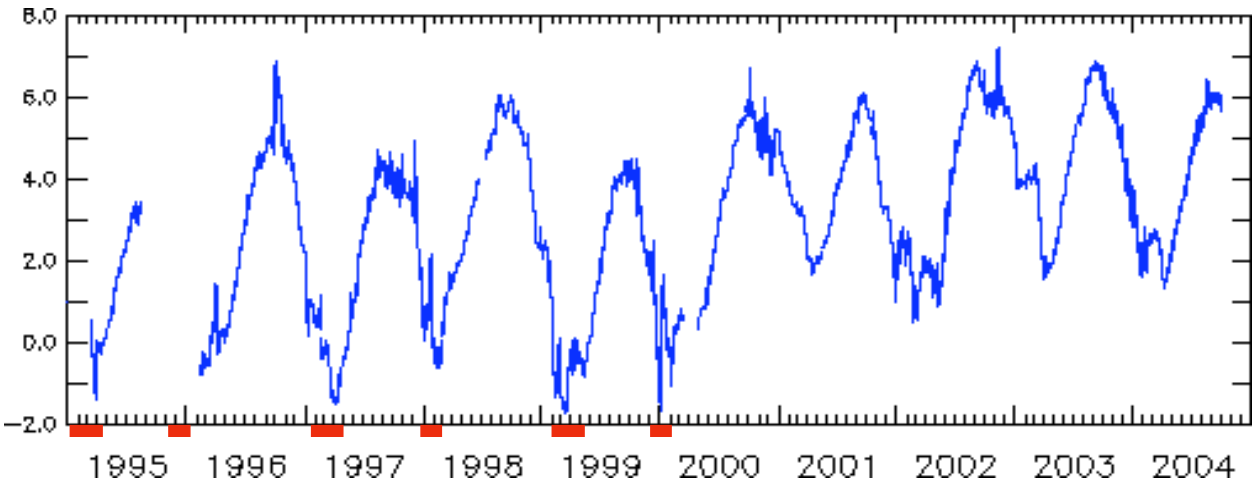

Figure 19. Depth integrated temperature at Mooring 2. The red lines at the bottom of the plot indicate when ice was present over the mooring.

The depth-averaged temperature at Mooring 2 (Figure 20) includes strong annual cycle, of course, but also a striking transition that occurred in 2000. During each winter from 1995 through 2000, ice was advected over the site cooling the water column. Beginning in 2001, ice (concentration greater than 10%) has not been over the mooring. This has been accompanied by a prominent warming of 3˚C in the winter and about 2˚C in the summer.

Sea surface temperature in May, when the southeastern Bering Sea is free of ice, appears to be a good predictor for summer bottom temperature. The correlation coefficient between May SSTs averaged over the southeastern Bering Sea (MaySST index) and mean bottom temperature for the same region is $r = 0.82$ ($P < 0.001$) for the period 1982-2003. Although May SST somewhat decreased in the past two years from its all-time maximum in 2003, it remains well above its long-term average value (Figure 21). Therefore, all indications are for a continuation of the warmth of the recent years through the summer of 2005.

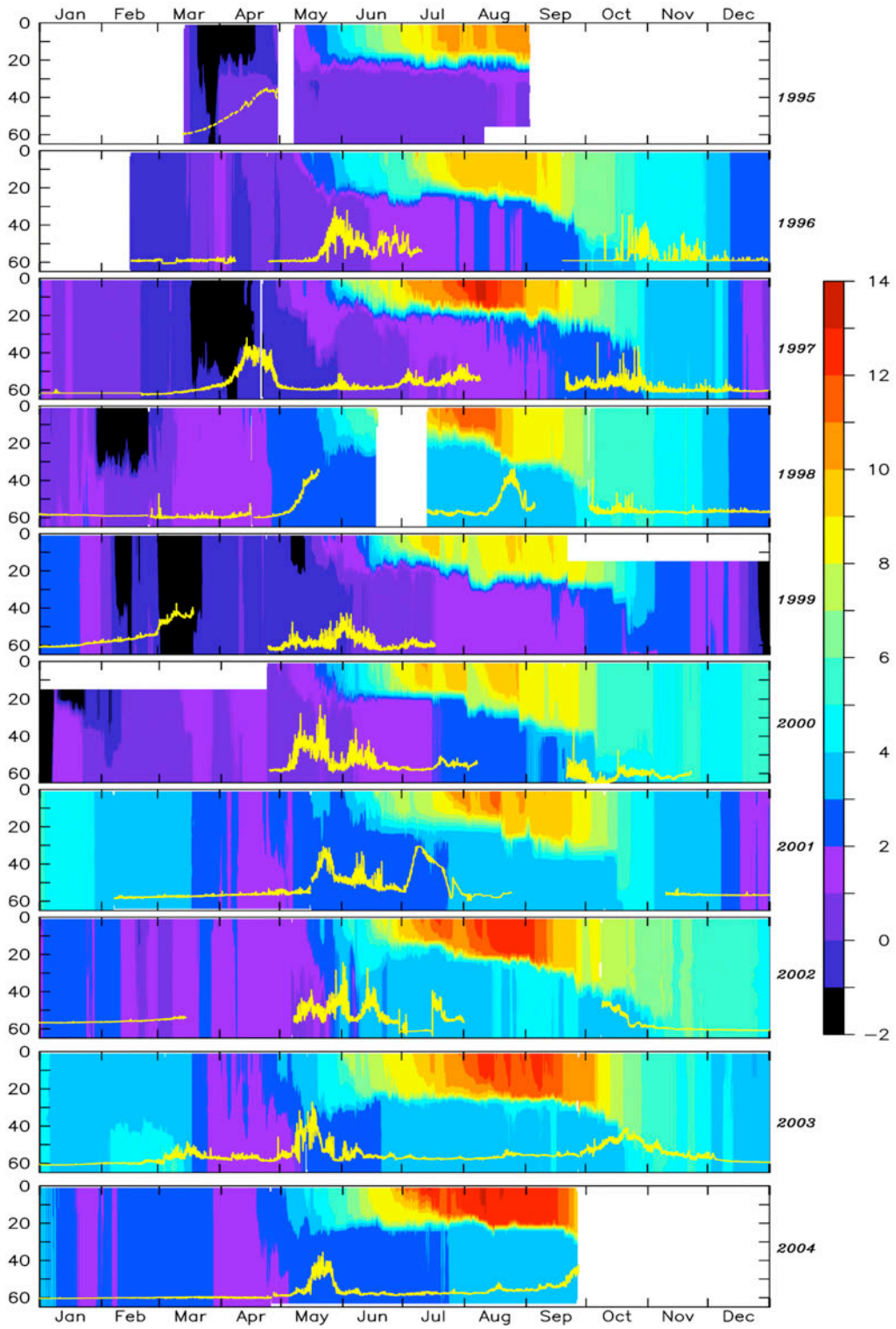

Figure 20. Contours of temperature measured at Mooring 2, 1995-2004. The coldest temperature (black) occurred when ice was over the mooring. The yellow line is fluorescence measured at ~11m. Note that early blooms are associated with the presence of ice.

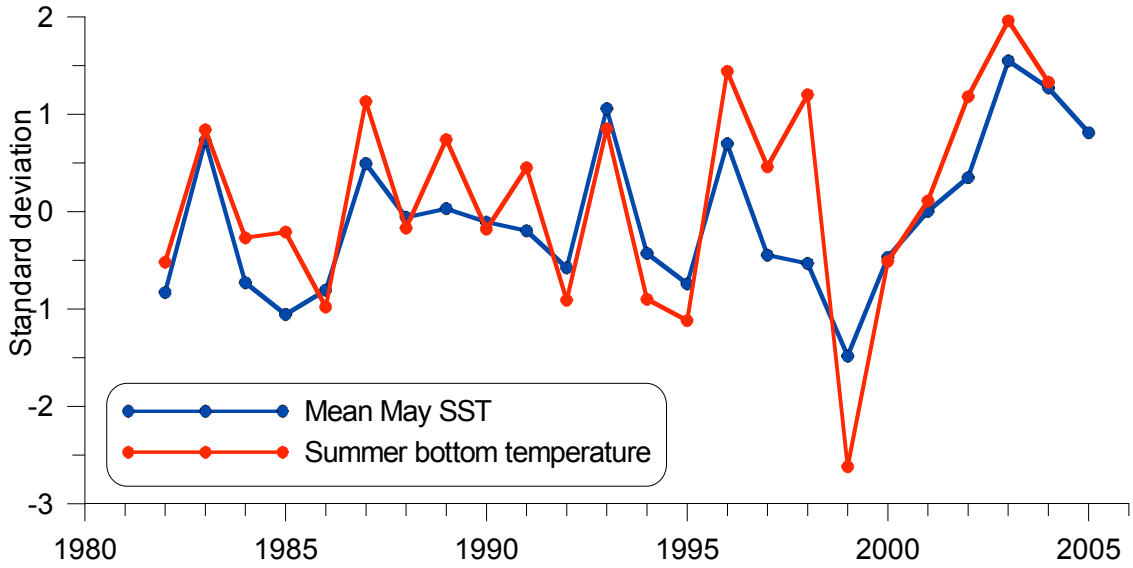

Figure 21. The MaySST index and mean summer bottom temperature in the southeastern Bering Sea, 1982-2005.

Simulated Drift Trajectories in the Southeast Bering Sea –FOCI
Contributed by Dylan Righi, FOCI, NOAA/PMEL
Last updated: November 2004

One of the most important resources in the Bering Sea (both for economic value and for its role in the ocean ecosystem) is the walleye pollock (*Theragra chalcogramma*) fishery. In the 1998, 50% of the world ocean catch of pollock came from the Bering Sea (Napp et al. 2000). At the same time walleye pollock (especially juveniles) are the main prey of other fishes, seabirds and marine mammals, meaning changes in stock size exert pressure on the entire Bering Sea food web. There are large inter-annual variations in pollock recruitment (Wespestad 1993) that must be understood in order to successfully manage this fishery. Climate variability and physical forcing play an important role in recruitment of fish and shellfish species (Wespestad et al. 2000; Wilderbuer et al. 2002; Zheng and Kruse 2000). Pollock recruitment is understood to be mainly set by their first year (Kendall and Duker 1998) and one fate that young pollock meet is cannibalism by adult pollock. Thus, transport of pollock eggs and larvae to regions of high adult density should adversely affect survival. Wespestad et al. (2000) test this hypothesis by using a surface transport model (OSCURS, (Ingraham and Miyahara 1988)) to simulate egg/larvae trajectories, and hindcasting survival rates. We attempt to improve on this work by using a full primitive equation ocean model to calculate trajectories instead.

We have used the northeastern Pacific Regional Ocean Model System (ROMS) to simulate trajectories in the southeastern Bering Sea. Drifter tracking in ROMS is done using a fourth order predictor-corrector scheme and allows vertical movement. We currently have results for the years 1996-2003. The simulated drifters are initialized in the Bering Sea just north of Unimak Island and to the northeast of Unimak Pass. This is known to be an area of spawning for walleye pollock (Hinckley 1987). The initial drifter positions fill out a seven by seven grid with horizontal separations of about 10 km (Figure 22). Vertically, there are 15 drifters initialized at each grid point with maximum depths just over 40 m. The drifter initial positions are denser near the surface, replicating vertical egg distribution data collected in the Bering Sea (Kendall et al. 1994). Drifters are released on April 1 of each year and are tracked for 90 days.

Endpoints after 90 days for drifter trajectories from the 1998-2003 runs are shown in Figure 23 (this plot shows all drifters at all depths). In all years there is a strong tendency for trajectories to move to the northeast up the Alaskan peninsula. The other common path is movement to the northwest along the 100-m isobath. The split between these two paths is seen clearly in the 1998, 1999, 2001 and 2003 drifter endpoints. The full trajectory plots (not shown here) show that the endpoints in 2000 are the result of a strong turning to the northwest of trajectories that had been moving up the Alaskan peninsula. In 2002 the drifters initialized at deeper points follow the common paths along the peninsula and the 100-m isobath. But drifters nearer the surface seem influenced by local winds and first move to the northeast, then turn to the northwest, resulting in endpoints spread evenly across the entire shelf. Further study of possible forcing mechanisms is needed to understand what leads to these years departing from the archetypal two-limbed flow.

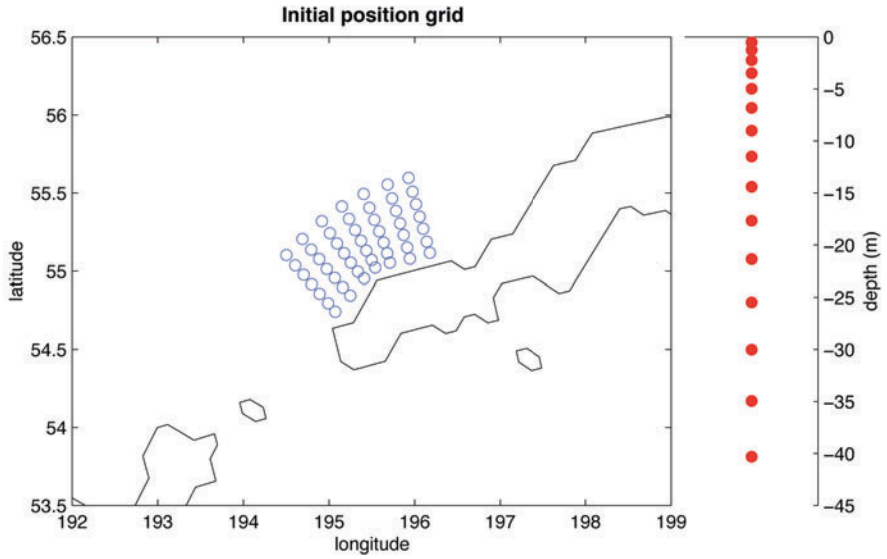

Figure 22. Simulated drifter initial horizontal (left) and vertical (right) positions.

The initial goal of this work was to compare simulated trajectories from a full primitive equation model with those from the Ocean Surface Current Simulations (OSCURS) numerical model. OSCURS computes daily surface current fields using daily sea level pressure and long-term mean geostrophic current data. As such, it is a simpler model in terms of the physics involved but is much more computationally inexpensive. Wespestad et. al. (2000) used OSCURS to create simulated trajectories in the Bering Sea. The initial grid used here was centered on the initial release point they used. Our trajectories for drifters released near the surface (0 to 5 m depth) show good agreement with the OSCURS results. But our results show variation of trajectory endpoints with changes in both horizontal and vertical initial position. Figure 24 shows the full trajectories for the 2001 simulated drifters. The upper left panel shows the tracks of all the drifters released, while the upper right and the bottom panels show drifter tracks as a function of their release depth. Within each depth bin it is evident that there is a large dependence of drifter endpoints on initial vertical placement with each bin showing, to relative degrees, the two-limbed split flow.

There is also a strong dependence on release depth. The OSCURS 2001 trajectory (not presented here) moves a short distance to the northeast up the Alaskan peninsula as do the majority of the

NEPROMS drifters released in the upper 5 m of the water column (upper right panel of Figure 24). But with deeper release points comes a stronger divergence of the trajectory fates. In the 5-20 m and 20-40 m release bins there are significant numbers of drifters that join the 100-m isobath flow to the northwest, with some even moving through Unimak Pass before turning back. OSCURS results would completely miss this variation in particle fates.

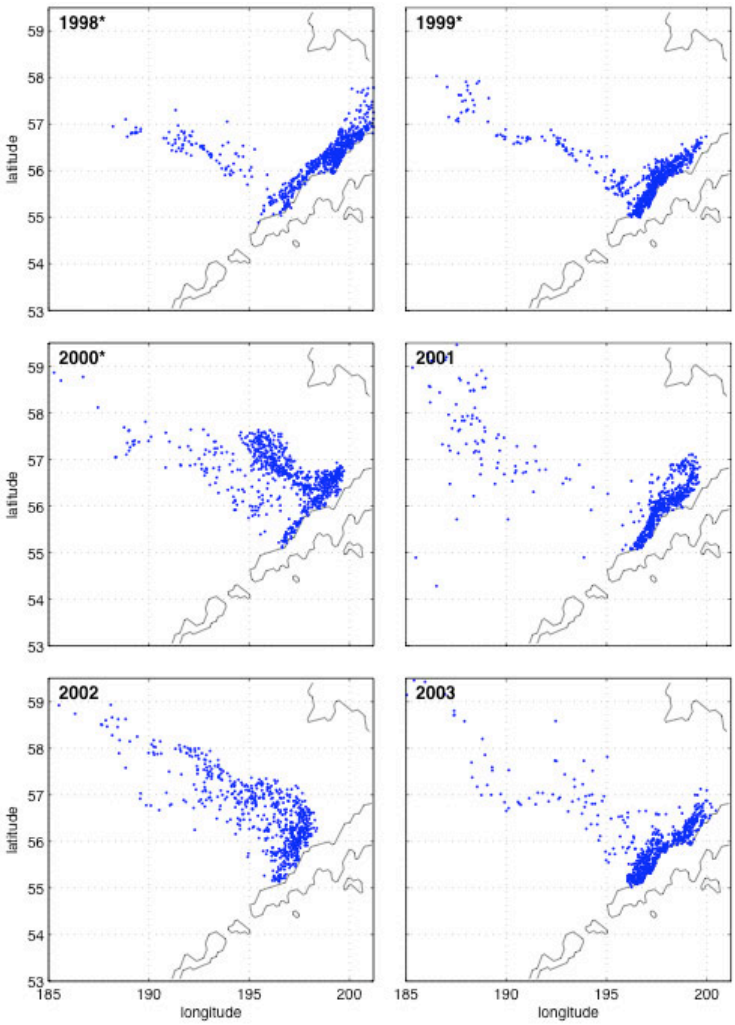

Figure 23. Endpoints for 90-day drifter trajectories for 1998-2003.

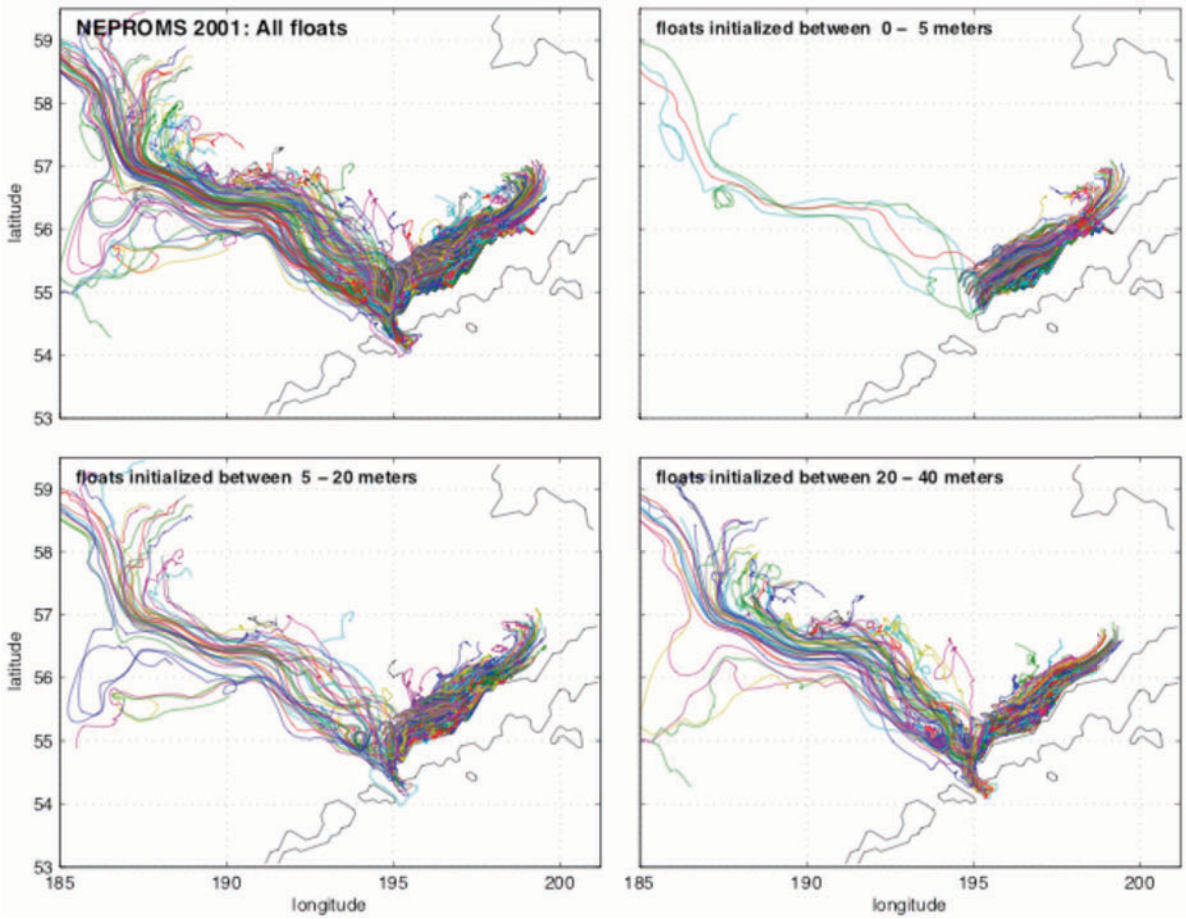

Figure 24. Full trajectories for the 2001 90-day simulated drifters. Upper left panel shows all drifters, while the upper left and bottom panels show drifters divided as a function of initial release depth.